Marine Pollution Bulletin 131 (2018) 515–524

Contents lists available at ScienceDirect

Marine Pollution Bulletin

journal homepage: www.elsevier.com/locate/marpolbul

Comparison of six digestion methods on fluorescent intensity and morphology of the fluorescent polystyrene beads

Fengmin Li[a,b], Fuyun Li[a,b], Xiaodong Hou[c], Xianxiang Luo[a,b], Haifeng Tu[a,b], Yadan Zou[a,b], Cuizhu Sun[a,b], Mei Shi[a,b], Hao Zheng[a,b,*]

[a] Institute of Coastal Environmental Pollution Control, and Ministry of Education Key Laboratory of Marine Environment and Ecology, Ocean University of China, Qingdao 266100, China
[b] College of Environmental Science and Engineering, Ocean University of China, Qingdao 266100, China
[c] Institute of Geochemistry, Chinese Academy of Sciences, Guiyang 550000, China

ARTICLE INFO

Keywords:
Fluorescent PS beads
Digestion
Fluorescence intensity
Morphology
Extraction efficiency

ABSTRACT

Effect of digestion methods on fluorescence intensity of fluorescent polystyrene (PS) beads was poorly understood, which may affect the accuracy of toxicity test of the fluorescent PS beads exposed to marine organisms. Therefore, six digestion approaches were compared on fluorescence intensities and properties of three commercial fluorescent PS beads. Among all the protocols, the digestion using KOH (10% w/v, 60 °C) (KOH-digestion) had no effect on the fluorescence intensity, morphology and composition of the three fluorescent PS beads. Moreover, the extraction efficiency ≥ 95.3 ± 0.2% of fluorescent PS beads in *Daphnia magna* and zebrafish, confirming its feasibility in fluorescent PS beads quantitative analysis. However, the fluorescence intensities of fluorescent PS beads digested by other five protocols were significantly decreased, as well as the change of morphology and composition on fluorescent PS beads. Overall, the KOH-digestion is an optimal protocol for extracting fluorescent PS beads in biological samples.

1. Introduction

Plastics are widely used around the world due to its light weight, long durability, strong plasticity, and low production cost (Ivar and Costa, 2014). Global virgin plastic production reached 8300 million metric tons as of 2017, and approximately 60% of all the plastics ever produced were discarded and are accumulated in landfills or in the natural environment (Geyer et al., 2017). Approximately, 4.8–12.7 million metric tons of plastic waste generated on land of 192 coastal countries in 2010 due to mismanagement entered into oceans (Jambeck et al., 2015). Plastics debris eventually fragment into powdery or microsized fragments in the beach and seawater environment, due to ultraviolet radiation and waves, typically not visible to the naked eye, are called microplastics (MPs), of which the size is < 5 mm (Barnes et al., 2009; Andrady, 2011). Occurrence of MPs in oceans has been reported throughout the world. For example, the mean abundance of MPs was 2080 ± 2190 items m^{-3} in the Pacific Ocean (Desforges et al., 2014). And the MPs (38–234 items m^{-3}) even appeared in the ice cores collected from remote locations in the Arctic Ocean (Obbard et al., 2014). The maximum concentrations of MPs have reached 100,000 items m^{-3} in Swedish harbour area adjacent to a polyethylene production plant (Noren and Naustvoll, 2010). Therefore, the fate and ecotoxicity effects of MPs in marine environment had become one of the hottest environmental issues (Kanhai et al., 2017).

Because of the small particle size and high content MPs are easily ingested by aquatic organisms such as copepods (Cole et al., 2013) and fish (Luís et al., 2015). Ingestion and accumulation of MPs can cause adverse effects on organisms, such as blocking alimentary canal (Wright et al., 2013), restricting food intake (Cole et al., 2013), causing neurotoxicity (Barboza et al., 2018), thus inhibiting body growth and development (Sussarellu et al., 2016). Furthermore, MPs can act as vectors for hydrophobic organic contaminants in aquatic environment because of their large surface area to volume ratio and hydrophobic properties (Ogata et al., 2009). As a result, it is important to investigate the ingestion of MPs by marine organisms and examine their impact on the organisms (Rist et al., 2017).

The fluorescent polystyrene (PS) beads are a type of artificially manufactured commercial plastic microbeads with stable fluorescence that enable a clear distinction from other environmental plastic particles (Cole et al., 2013; Watts et al., 2016). And the fluorescent PS beads

* Corresponding author at: Institute of Coastal Environmental Pollution Control, and Ministry of Education Key Laboratory of Marine Environment and Ecology, Ocean University of China, Qingdao 266100, China.
E-mail address: zhenghao2013@ouc.edu.cn (H. Zheng).

https://doi.org/10.1016/j.marpolbul.2018.04.056
Received 7 February 2018; Received in revised form 23 April 2018; Accepted 24 April 2018

Table 1
The details of six selected digestion protocols for extracting fluorescent PS beads.

Reagents	Concentration[a]	Volume[b] (mL)	Temperature[c] (°C)	Duration time[d] (h)	References
KOH	10% (w/v)	40.0	60	24	Dehaut et al., 2016
NaOH	10 M	40.0	60	24	Cole et al., 2014
H_2O_2	30% (w/w)	40.0	65	24	Li et al., 2015
HNO_3	69% (w/w)	1.0	70	2	Lu et al., 2016
HNO_3:HCl	1:1 (v/v)	1.0	80	1/2	Desforges et al., 2014
HNO_3:$HClO_4$[e]	4:1 (v/v)	1.0	20/90	12/(1/6)	De Witte et al., 2014

[a] 10% (w/v) indicated the concentration of KOH was 100 g L^{-1}; 30% and 69% (w/w) indicated the mass fraction of H_2O_2 and HNO_3 was 30% and 69%, respectively; 1:1 (v/v) and 4:1 (v/v) indicated the volume ratio of HNO_3:HCl and HNO_3:$HClO_4$ was 1:1 and 4:1, respectively, and the mass fraction of HCl and $HClO_4$ was 37% and 71%.
[b] Volume indicated the amount of the reagent that used in the digestion.
[c] Temperature indicated the constant temperature during digestion.
[d] Duration time indicated the duration time used in the digestion.
[e] The fluorescent PS beads were digested using HNO_3:$HClO_4$ at 20 °C for 12 h, then at 90 °C for 1/6 h.

are often used in laboratory toxicity experiments to investigate their accumulation and transfer in marine organisms (Lu et al., 2016; Rist et al., 2017). Thus the quantification of fluorescent PS beads ingested by organisms is crucial to assess their potential impacts to marine ecosystems. One of the commonly used quantitative methods of fluorescent PS beads ingested by organisms is the observation of the tissue sections using fluorescence microscopy (Batel et al., 2016). However, this method is less applicable for quantifying fluorescent PS beads ingested by organisms, because it is complex, time-consuming, and are likely to cause omission of fluorescent PS beads (Rist et al., 2017). Additionally, quantification using fluorescence microscopy is limited by the particle size of fluorescent PS beads and the resolution of the microscope (Rist et al., 2017). Consequently, a viable quantitative method via measuring the fluorescence intensity of the fluorescent PS beads has been used to determine the content of MPs in biological samples (Rosenkranz et al., 2009; Lu et al., 2016). Nevertheless, the measurement of fluorescence intensities of the fluorescent PS beads was based on thoroughly digestion of the biological samples (Rist et al., 2017). Studies had shown that the digestion reagent such as strong acidic (e.g., HCl, HNO_3, and $HClO_4$) and alkali (e.g., NaOH and KOH) solution, strong oxidizing reagent (e.g., H_2O_2), and Protease K could effectively remove the organic matters from the biological samples (Lusher et al., 2017). Among these methods, the protease K was not recommended because of its complicated procedures and lower extraction efficiency (Dehaut et al., 2016). Moreover, the extraction efficiency of fluorescent PS beads was also related to the digestion conditions and the chemical resistance. However, little was known about the effect of the digestion approaches on the fluorescence intensity and extraction efficiency of fluorescent PS beads in the biological samples.

Therefore, six digestion reagents were selected to study the effect of different digestion approaches on the fluorescence intensity, surface morphology, and extraction efficiency of three common commercial fluorescent PS beads. The specific objectives were to: (1) investigate the effects of the six published digestion methods that commonly used in literatures on the fluorescence intensity and morphology of fluorescent PS beads; (2) explore the effects of the volume of the digestion reagents, digestion temperature and duration time on the fluorescence intensities of fluorescent PS beads; (3) evaluate the extraction efficiency of fluorescent PS beads in the biological samples by the optimal method; and (4) elucidate the underlying mechanisms responsible for the decreased fluorescence intensity of fluorescent PS beads resulted from the digestion protocols. These findings will screen an optimal digestion protocol for quantitative analysis of the fluorescent PS beads in the biological samples using fluorescence spectrophotometer, which is helpful for investigating and predicting the ecotoxicity effects of fluorescent PS beads in marine ecosystems.

2. Materials and methods

2.1. Fluorescent PS beads preparation

Three kinds of fluorescent PS beads were purchased from Thermo Fisher Scientific (MA, United States), Baseline ChromTech Research Centre (Tianjin, China), and Big Goose ChromTech Research Centre (Tianjin, China), respectively. The properties of the pristine fluorescent PS beads were shown in Table S1. All of the stock solutions were dispersed in 2 L Milli-Q water and sonicated for 15 min at 120 W (FB 120, Fisher Scientific, USA) to avoid aggregation. The composition of the pristine fluorescent PS beads without treatment was confirmed by Fourier transform infrared spectroscopy with attenuated total reflectance accessory (ATR-FTIR, L1600401, Spectrum, UK), and there was no significant difference in the composition of the pristine fluorescent PS beads (Fig. S1).

2.2. Digestion and determination of the fluorescent PS beads

Six digestion methods were selected according the published studies to investigate their effects on fluorescence intensity of the fluorescent PS beads, and each group set 3 parallels. Briefly, the fluorescent PS beads (1.0 mg) and the desired volume of digestion solution were added to 10 mL or 100 mL glass bottles with caps to avoid contamination. Then, the samples were digested in a constant temperature water bath. The specific procedures for the six digestion methods were shown in Table 1. Subsequently, the pristine fluorescent PS beads and digested fluorescent PS beads were diluted with Milli-Q water to a final volume of 100 mL and the fluorescence intensity was measured using a fluorescence spectrophotometer (F-4600, Hitachi, Japan).

To investigate the effect of digestion conditions including volume of the digestion reagent, digestion temperature, and duration time on the fluorescence intensities of fluorescent PS beads, the experiments were divided into three groups and each group was set for triplicates. In the first group, the effect of the digestion reagent volume on the fluorescence intensity of fluorescent PS beads was explored. The volumes for these reagents are shown in Table S2, i.e., HNO_3: 0.2–1.5 mL, HNO_3:HCl: 0.2–1.4 mL, HNO_3:$HClO_4$: 0.5–2.0 mL, H_2O_2: 2.0–90 mL, NaOH: 10–60 mL and KOH: 10–60 mL, the digestion temperature was 60 °C and duration time was 24 h. In the second group, the effect of the digestion temperature from 20 °C to 90 °C on the fluorescence intensity of fluorescent PS beads was investigated. The volumes of HNO_3, HNO_3:HCl, HNO_3:$HClO_4$ were 10 mL and the volumes of H_2O_2, NaOH and KOH were 60 mL, the fluorescence intensity of the fluorescent PS beads had reached a steady state in the above volumes, and the duration time was 24 h. In the third group, the effect of the duration time from 10 min to 72 h on the fluorescence intensity of fluorescent PS beads was compared. The digestion reagent volumes were same as the

second group, and the digestion temperature was 60 °C. Besides, the detailed changes of digestion reagent volume, digestion time and digestion temperature were presented in Table S2. After digestion, the fluorescence intensities of the digested fluorescent PS beads was measured as aforementioned.

2.3. Characterization of fluorescent PS bead samples

After digestion, the fluorescent PS beads solution was dropped onto a blood cell count plate and observed the changes of fluorescence under a fluorescence microscope (FEICA DM-2500) at a magnification of 20 times. The remaining fluorescent PS beads solution was filtered using a 0.45 μm mixed-fiber membrane, and the fluorescent PS beads remained on the membrane was lyophilized for 3 days. Then, the fluorescent PS beads were identified by ATR-FTIR to determine the changes of the functional groups. And the remaining fluorescent PS beads were examined using scanning electron microscopy (SEM, JSM-6390LV, JEOL, Japan).

2.4. Extraction efficiency of fluorescent PS beads in biological samples

Based on the above studies, the optimal digestion method which has no/little impact on the fluorescence intensities of digested fluorescent PS beads was applied to extract the fluorescent PS beads in the biological samples, and to verify the reliability of the screened method by calculating their extraction efficiency. The *Daphnia magna* (*D. magna*) and zebrafish were chosen as the tested organisms, which had been cultured in our laboratory for over three months. They were starved for 24 h before the experiments to allow full gut depuration.

In the first experiment, the pristine fluorescent PS beads were simply mechanically mixed with *D. magna* or zebrafish to determine the extraction efficiency. In brief, one hundred individuals of *D. magna* or a zebrafish (20 ± 5 mg) was executed and homogenized, then added into a glass bottle containing 2 mg spiked pristine fluorescent PS beads. The spiked pristine fluorescent PS beads were diluted, measured the fluorescence intensity and calculated the concentration (C_0) using the standard curve of pristine fluorescent PS beads (Fig. 1F) before adding into the glass bottle. The content of the spiked pristine fluorescent PS beads was calculated and recorded as Q_0. Subsequently, this mixture was digested using KOH-digestion at 60 °C for 72 h and the fluorescence intensity of the mixture solution after digestion was measured and the concentration of fluorescent PS beads (C_m) was calculated according to the standard curve (Fig. 1F). Thus the content of fluorescent PS beads after digestion (Q_m) was calculated. The extraction efficiency (R_m) of the fluorescent PS beads mechanically mixed with *D. magna* or zebrafish was calculated as following:

$$R_m = \mathrm{Q_m}/Q_0 \times 100\%.$$

In the second experiment, the *D. magna* or zebrafish was exposed to the pristine fluorescent PS beads solution to confirm the extraction efficiency. In detail, one hundred *D. magna* or a zebrafish after depuration for 24 h was randomly added into a 100 mL beaker containing 40 mL Mili-Q water and 2 mg fluorescent PS beads, then cultured in a constant temperature incubator (25 °C, light: dark = 12: 12) for 24 h. After the exposure, the *D. magna* or zebrafish was collected and rinsed with Mili-Q water three times to remove the adhered pristine fluorescent PS beads from these organisms. Each treatment was set for triplicates. The exposed organisms were homogenized and digested as the first recovery experiment. Subsequently, the fluorescence intensity was measured and the content of fluorescent PS beads ingested by *D. magna* and zebrafish was calculated and recorded as Q_{i-1}. Besides, the fluorescence intensity of the fluorescent PS beads remained in the Mili-Q water without digestion was also measured and the content Q_{i-2} was calculated. Thus the extraction efficiency (R_i) of the fluorescent PS beads ingested by *D. magna* or zebrafish was calculated as following:

$$Q_i = Q_{i-1} + Q_{i-2}$$

$$R_i = Q_i/Q_0 \times 100\%$$

The blank was set as follow: one hundred individuals of *D. magna* or a zebrafish was executed and homogenized. Subsequently, the homogenate was digested by KOH-digestion as above, and zeroing the fluorescence intensity with the digestion solution before measuring the fluorescence intensity of fluorescent PS beads both mechanically mixed and ingested by the organisms.

2.5. Data analysis

The results were expressed as mean values ± standard deviation ($n = 3$). The significance of the various parameters was tested by one-way analysis of variance (ANOVA) using Turkey HSD test and the correlation was analyzed using Pearson test (two-tailed) at $P < 0.05$ for the control and digested groups. All of the analyses were performed using Statistical Product and Service Solutions (SPSS, 20.0). A P value < 0.05 was accepted as significant difference.

3. Results

3.1. Effects of the digestion methods on the fluorescence intensities of fluorescent PS bead

The fluorescence intensities of the fluorescent PS beads digested by the six selected protocols (Table 1) were shown in Fig. 1. Obviously, the concentrations and fluorescence intensities of the pristine fluorescent PS beads were significantly linearly correlated. After the acid-digestion using HNO_3, HNO_3:HCl, and HNO_3:$HClO_4$, the fluorescence intensity sharply decreased by 97.7–99.9% (Fig. 1A–C). However, the H_2O_2-digestion had no effect on the fluorescence intensity at the lower concentration of fluorescent PS beads ($< 3\ mg\ L^{-1}$), while significantly decreased the fluorescence intensity by 6.65–17.7% at the higher concentration ($\geq 5\ mg\ L^{-1}$, Fig. 1D). On the contrary, the alkali-digestion using NaOH (Fig. 1E) and KOH (Fig. 1F) had less effect on the fluorescence intensity compared to those of the acid- or H_2O_2-digestion. Moreover, the KOH-digestion had less effect on the fluorescence intensity relative to the NaOH-digestion (0.51–3.06% vs 3.24–16.3%). Similarly, for the other two fluorescent PS beads, the six digestion protocols showed the similar effects on the fluorescence intensities (Figs. S2–3).

3.2. Effect of the digestion reagent volumes on the fluorescence intensities of fluorescent PS beads

The effect of the digestion reagent volumes on the fluorescence intensities of fluorescent PS bead was shown in Fig. 2. For the HNO_3-digestion, the fluorescence intensities of fluorescent PS beads at lower volume (0.2 mL) of digestion reagent were significantly higher than those of the higher volume (0.5–1.5 mL) treatments (Fig. 2A). For the HNO_3:HCl-digestion, the fluorescence intensities of fluorescent PS beads decreased with increasing volume of the digestion reagents (Fig. 2B). Inconsistently, for the HNO_3:$HClO_4$-digestion, the fluorescence intensities showed an increasing tendency with the increasing volume of the digestion reagent when the fluorescent PS beads concentration was lower than $8\ mg\ L^{-1}$, but the fluorescence intensities significantly decreased with the increasing volume of the digestion reagent when the concentration of fluorescent PS beads was at $10\ mg\ L^{-1}$ (Fig. 2C). Generally, the fluorescence intensities of the fluorescent PS beads were significantly decreased after the acid-digestion even using the lowest volume of digestion reagents when compared with pristine fluorescent PS beads. For the H_2O_2- and NaOH-digestion, the fluorescence intensity slightly changed when the reagent volume increased, but the fluorescence intensity of the fluorescent PS beads was basically stable when the volumes of H_2O_2 and NaOH reached 40 mL

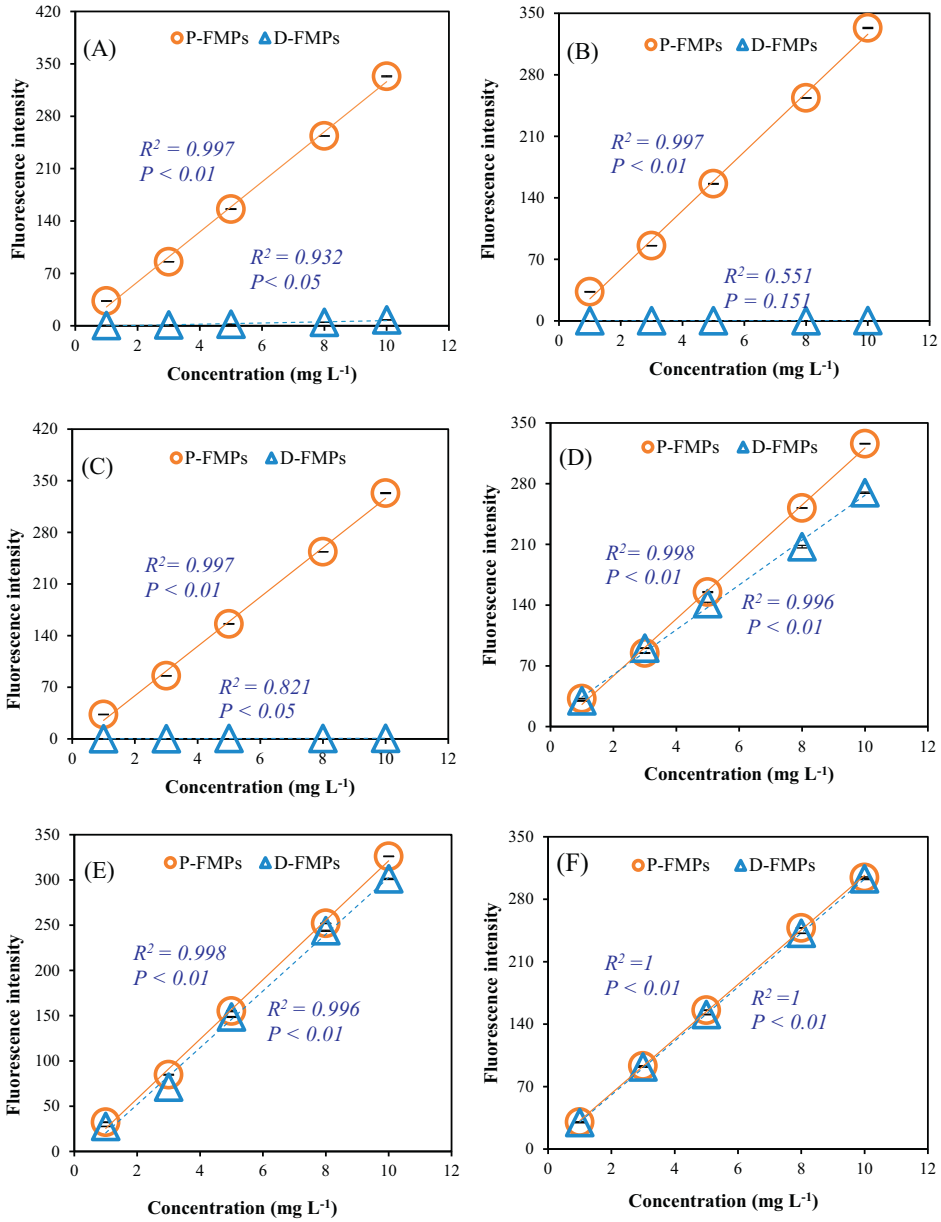

Fig. 1. Effect of the selected digestion methods on the fluorescence intensities of the fluorescent PS beads bought from Thermo Fisher Scientific. The digestion conditions are shown in Table 1. P-FMPs and D-FMPs indicated the pristine and digested fluorescent PS beads, respectively. (A) HNO_3; (B) HNO_3:HCl; (C) HNO_3:$HClO_4$; (D) H_2O_2; (E) NaOH; (F) KOH. The error bars are standard deviation (n = 3).

and 50 mL, respectively (Fig. 2D–E). However, there were no significant differences in the fluorescence intensities of the fluorescent PS beads digested using different volumes of KOH solution (Fig. 2F). For the other two fluorescent PS beads, the fluorescence intensities showed the similar volume-dependent response to these six digestion reagents (Figs. S4–5).

3.3. Effect of the digestion temperature and duration time on the fluorescence intensities of fluorescent PS beads

The effect of the digestion temperature on the fluorescence intensities of the fluorescent PS beads bought from Thermo Fisher Scientific was presented in Fig. 3A. For the acid-digestion using HNO_3, HNO_3:HCl, and HNO_3:$HClO_4$, the fluorescence intensities of the digested fluorescent PS beads decreased by 33.5%, 94.5% and 47.3% at 20 °C when compared with the pristine fluorescent PS beads, and the fluorescence intensities decreased by 91.5–99.9%, 99.8–99.9% and 74.7–99.6%, respectively when the temperature increased from 40 to 90 °C. For the H_2O_2-digestion, the fluorescence intensities showed fluctuation state with 13.3–42.0% reductions as the digestion temperature increased from 20 to 90 °C. For the NaOH- or KOH-digestion, the fluorescence intensities of the digested fluorescent PS beads slightly decreased by 2.08–7.76% and 3.95–6.00% compared to the pristine fluorescent PS beads with temperature increasing from 20 to 70 °C, respectively. However, when the temperature reached above 80 °C, the fluorescence intensities of digested fluorescent PS beads decreased by 19.8–20.1% for NaOH and 10.7–13.6% for KOH compared with the pristine fluorescent PS beads. Besides, the effects of digestion temperature on the fluorescence intensities of the other two fluorescent PS beads were consistent with this one (Fig. 3C, E).

The effect of digestion duration time on the fluorescence intensities of the fluorescent PS beads was shown in Fig. 3B. Compared with the pristine fluorescent PS beads, the acid-digestion using HNO_3, HNO_3:HCl, and HNO_3:$HClO_4$ decreased the fluorescence intensities of

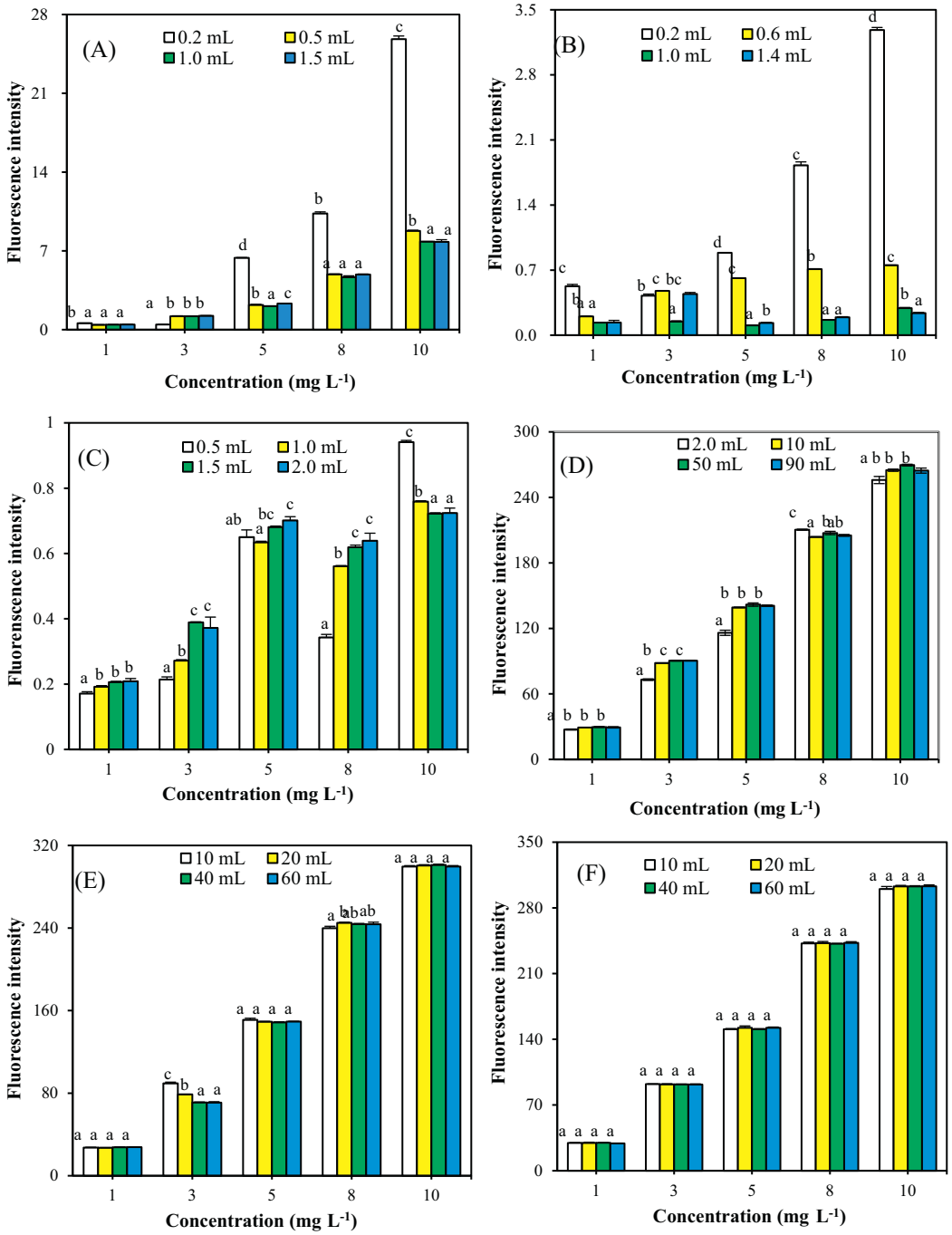

Fig. 2. Effect of the digestion reagent volumes on the fluorescence intensities of the fluorescent PS beads bought from Thermo Fisher Scientific. The digestion temperature and duration time was 60 °C and 24 h, respectively. (A) HNO_3; (B) HNO_3:HCl; (C) HNO_3:$HClO_4$; (D) H_2O_2; (E) NaOH; and (F) KOH. Different small letters indicated significant difference among the treatments with different volumes of the digestion reagents, which was analyzed by Turkey HSD test ($P < 0.05$) using SPSS 20.0.

fluorescent PS beads by 99.7%, 99.9% and 99.9% respectively when digested for 10 min, and the remained fluorescence intensity almost unchanged with increasing digestion time. In the H_2O_2-digestion, the fluorescence intensities decreased by 1.91% to 66.0% as the digestion time increased from 10 min to 72 h. For the NaOH-digestion, the fluorescence intensities only decreased by 0.72% to 4.76% as the duration time increased from 10 min to 72 h. However, in the KOH-digestion, as the duration time increased, no changes were observed for the fluorescence intensities of the fluorescent PS beads compared to the pristine ones. Moreover, the changes of fluorescence intensity of the other two fluorescent PS beads upon these digestion with different duration time showed the consistent pattern (Fig. 3D, F).

3.4. Effect of the digestion methods on morphology of the fluorescent PS beads

The pristine fluorescent PS beads were well monodisperse with strong fluorescence intensity (Fig. 4A). After the acid-digestion using HNO_3, HNO_3:HCl, and HNO_3:$HClO_4$, their fluorescence intensities markedly decreased, and the fluorescent PS beads aggregated. However, the H_2O_2-, NaOH-, and KOH-digestion had little effect on the fluorescence intensities, and the fluorescent PS beads were well

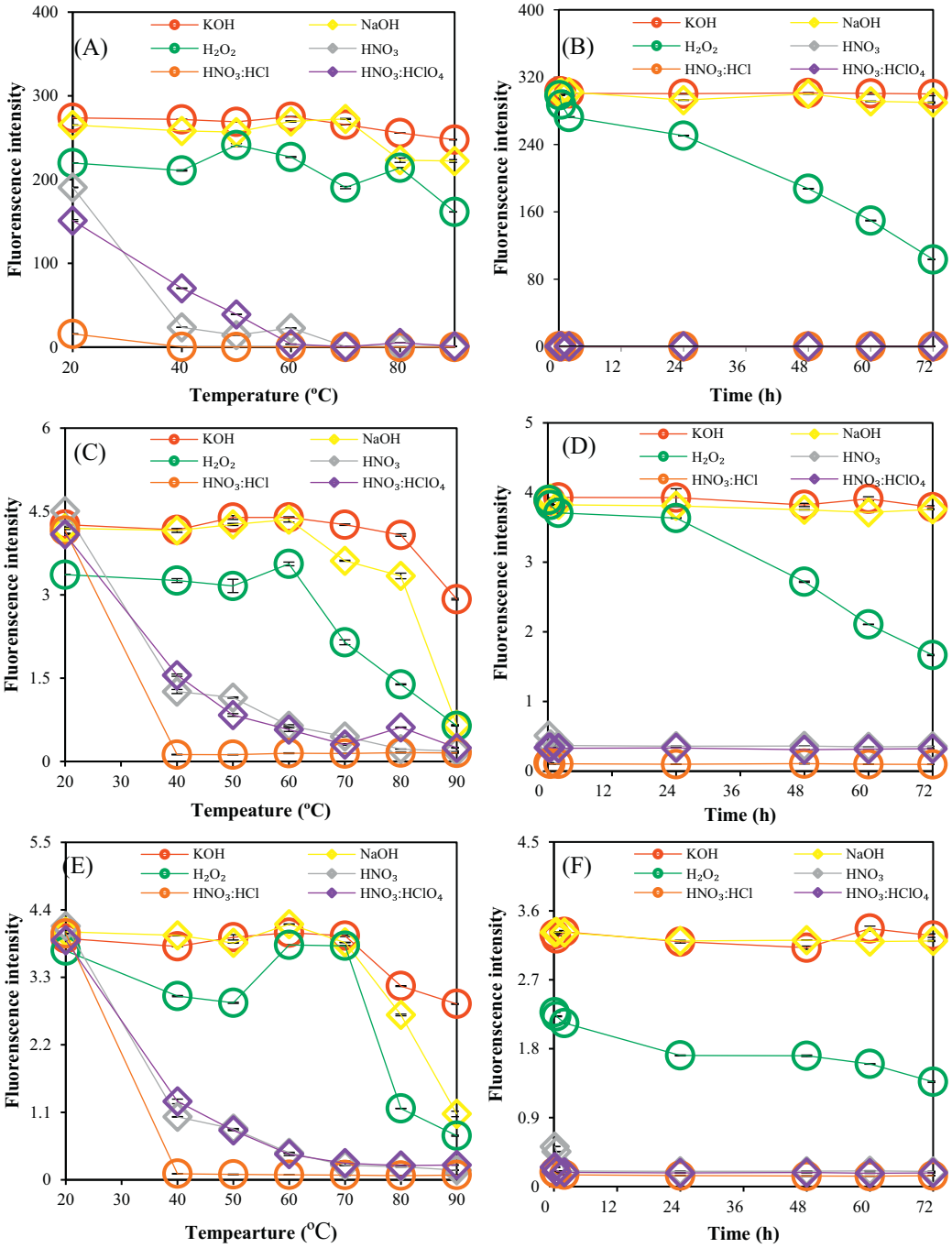

Fig. 3. Effects of the digestion temperature (left column, duration time was 24 h) and duration time (right column, digestion temperature was 60 °C) on the fluorescence intensities of the fluorescent PS beads bought from Thermo Fisher Scientific (A, B), Baseline ChromTech Research Centre (C, D) and Big Goose ChromTech Research Centre (E, F). The volumes of HNO_3, HNO_3:HCl, HNO_3:$HClO_4$, H_2O_2, NaOH and KOH were 10, 10, 10, 60, 60, and 60 mL, respectively.

dispersed (Fig. 4E–G). For the other two kinds of domestic fluorescent PS beads, these digestion methods showed the similar influences on their surface morphology (Figs. S6–7). Specifically, for the fluorescent PS beads bought from Big Goose ChromTech Research Centre digested by HNO_3:HCl and HNO_3:$HClO_4$, their fluorescence intensities disappeared completely, and the fluorescent PS beads bought from Big Goose ChromTech Research Centre can only be observed by turning the fluorescence microscope into a bright field of view (Fig. S7C–D).

The FTIR spectra showed that the pristine fluorescent PS beads were typical PS beads with characteristics functional groups (Fig. 5, Figs. S8–9). The band at 3026 cm^{-1} was assigned to the stretching mode of the aromatic C—H bonds and the bands at 2924 cm^{-1} were the C—H stretching vibration of PS (Torres et al., 2007). The bands at 1601 and 1452 cm^{-1} were the aromatic C=C stretching (Yu et al., 2014), and 1026 cm^{-1} was the bending mode of the C—H bonds in the aromatic ring (Wang et al., 2017). In addition, the bonds of the C—H on the aromatic ring out of plane was at 758 and 698 cm^{-1} and C—C skeleton stretching vibration for phenyl ring was at 540 cm^{-1} (Rebollar et al., 2008; Wang et al., 2017). The functional groups of the three digested fluorescent PS beads which were digested by HNO_3, HNO_3:HCl, and HNO_3:$HClO_4$ were identical, but they were different from the pristine fluorescent PS beads. New chemical bonds including C=O at 1650 and 1276 cm^{-1}, C—O stretching at 1092 cm^{-1} and O—H stretching vibrations at 839 cm^{-1} were observed on the digested fluorescent PS beads

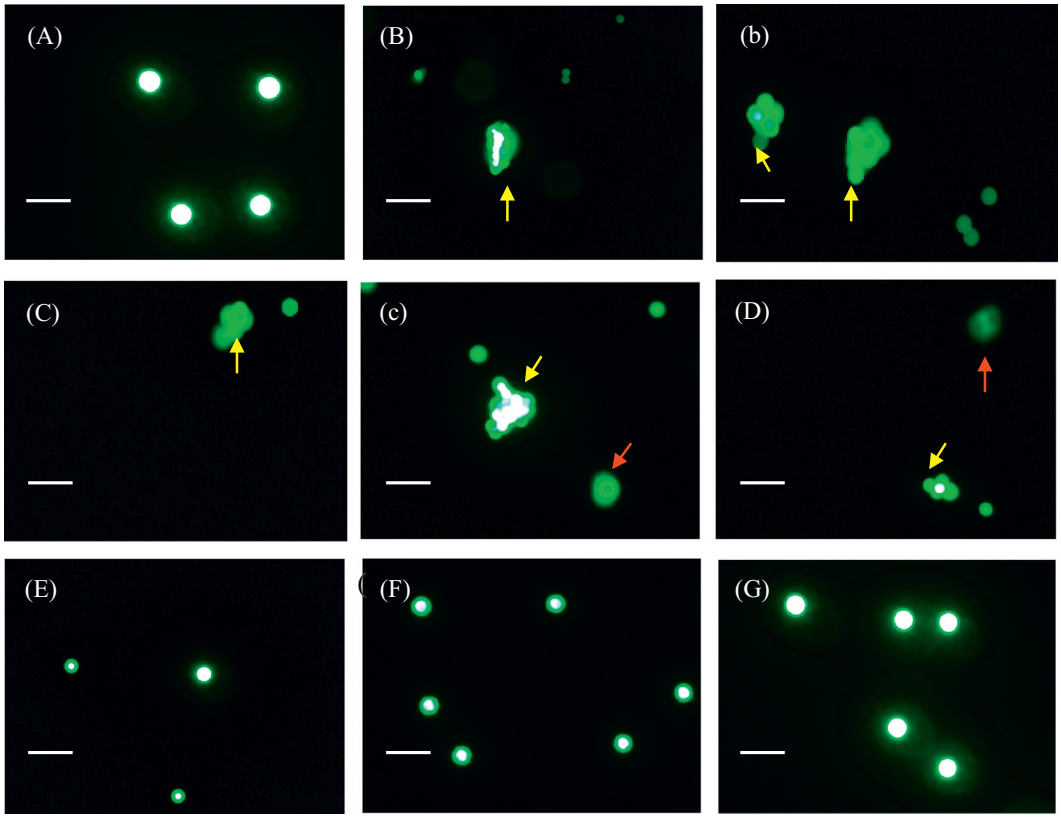

Fig. 4. Photographs of the pristine (A) and digested fluorescent PS beads bought from Thermo Fisher Scientific using (B, b) HNO_3; (C, c) HNO_3:HCl; (D) HNO_3:$HClO_4$; (E) H_2O_2; (F) NaOH; and (G) KOH, respectively. The digestion conditions are shown in Table 1. Compared with the pristine fluorescent PS beads (A), the fluorescence intensities of fluorescent PS beads after the acid-digestion using HNO_3 (B), HNO_3:HCl (C) and HNO_3:$HClO_4$ (D) distinctly decreased, and the fluorescent PS beads aggregated (the yellow arrows). Moreover, the fluorescent chemicals leaked from the fluorescent PS beads (the red arrows). However, the H_2O_2-, NaOH-, and KOH-digestion had little effect on the fluorescence intensities, and the fluorescent PS beads were well dispersed (Fig. 4E–G). (For interpretation of the references to colour in this figure legend, the reader is referred to the web version of this article.)

using HNO_3, HNO_3:HCl, and HNO_3:$HClO_4$ (Cui et al., 2015; Luo et al., 2017; Yang et al., 2017). However, no difference in the functional groups was observed between the pristine and digested fluorescent PS beads by using H_2O_2 or alkali-digestion.

The SEM images of these digested fluorescent PS beads were shown in Fig. 6. The pristine fluorescent PS beads showed a state of uniform dispersibility, and the surface of these particles was smooth (Fig. 6A). However, after the acid-digestion using HNO_3, HNO_3:HCl, and HNO_3:$HClO_4$, a series of mechanical damages were appeared on their surface, such as agglomeration, bubbles, shallow scratches, and deep depressions (Fig. 6B–D). Slight damages and aggregations appeared on the surface of the digested fluorescent PS beads using H_2O_2 (Fig. 6E). Moreover, stronger aggregations appeared on the surface of digested fluorescent PS beads by the NaOH-digestion (Fig. 6F1). However, after the KOH-digestion, the digested fluorescent PS beads dispersed homogeneously relative to the pristine fluorescent PS bead with no changes on the surface (Fig. 6G). The SEM images of the other domestic fluorescent PS beads were consistent with fluorescent PS beads bought from Thermo Fisher Scientific (Figs. S10–11).

3.5. Extraction efficiency of the fluorescent PS beads in the biological samples using the KOH-digestion

The extraction efficiency of the fluorescent PS beads bought from Thermo Fisher Scientific using the KOH-digestion at 60 °C for 72 h was shown in Table 2. The KOH-digestion had a relatively high efficiency for extracting fluorescent PS beads from biological samples of zebrafish and *D. magna*. The extraction efficiency of the fluorescent PS beads mechanically mixed with the zebrafish and *D. magna* was 99.5 ± 0.9% and 99.6 ± 0.7%, respectively. Moreover, the efficiency of the fluorescent PS beads ingested by the zebrafish and *D. magna* was 95.7 ± 0.2% and 95.3 ± 0.2%, respectively.

4. Discussion

4.1. Effect of the digestion methods on fluorescent PS beads

Among the six selected protocols, the KOH-digestion had little impacts on the fluorescence intensity (Fig. 1F) and morphology (Fig. 6G) of the fluorescent PS beads compared with the pristine ones. Moreover, the extraction efficiency of fluorescent PS beads that mechanically mixed or ingested by the organisms after KOH-digestion were over than 95.3 ± 0.2% (Table 2). These results suggested that the KOH-digestion was a feasible and credible approach for extracting and quantifying fluorescent PS beads in the biological samples. However, the other five digestion methods decreased the fluorescence intensity (Fig. 1A–E) and changed the characteristics of the fluorescent PS beads with varying degrees (Fig. 6B–F). Consequently, the accumulation and pollution levels of fluorescent PS beads in organisms would be underestimated by these five digestion methods, especially for the acid-digestion, which almost eliminated all the fluorescence intensities of the fluorescent PS beads. For example, the uptake and accumulation of the fluorescent PS beads in zebrafish were probably underestimated by Lu et al. (2016) reported, who used HNO_3-digestion (70 °C, 2 h) to extract fluorescent PS beads from zebrafish tissues.

Our results also showed that the chemical digestion may affect the morphology of fluorescent PS beads, such as scratches, folds, damages and aggregation (Fig. 6). Although plastics are polymers with the

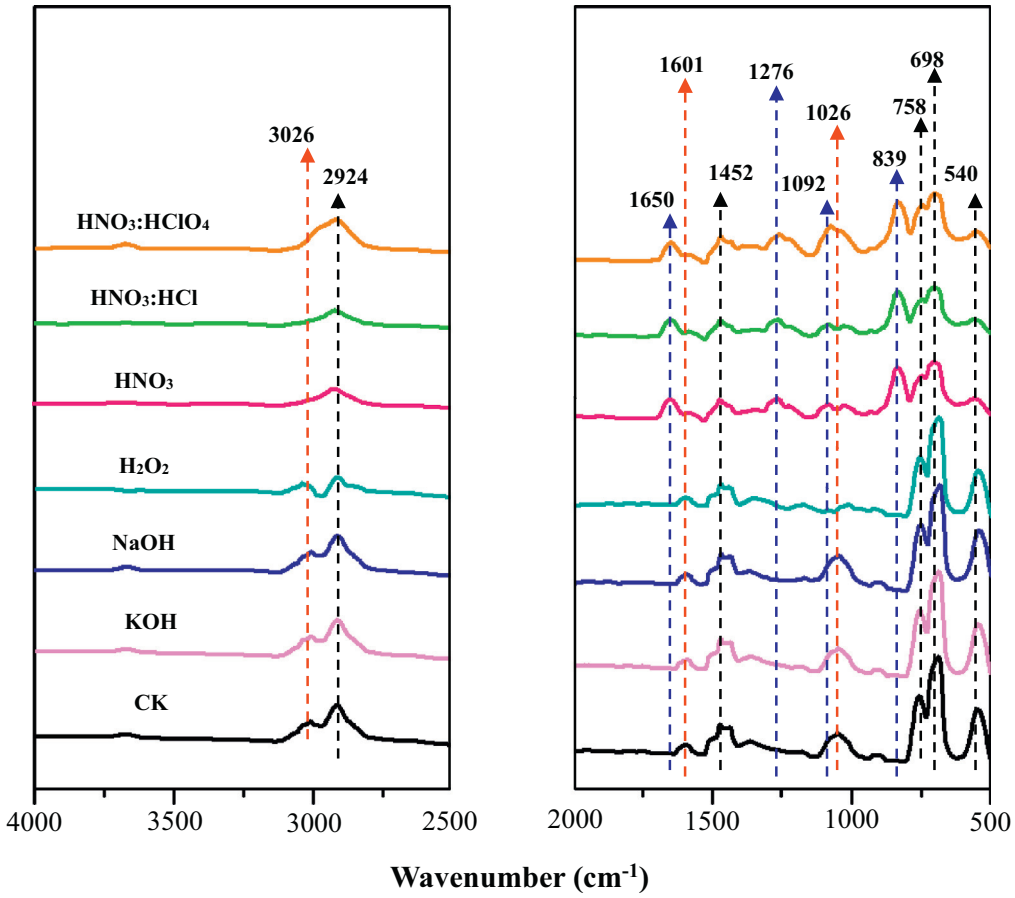

Fig. 5. The ATR-FTIR spectra of the pristine fluorescent PS beads (CK) and digested fluorescent PS beads according to the methods shown in Table 1 using KOH; NaOH; H_2O_2; HNO_3; HNO_3:HCl, and HNO_3:$HClO_4$, respectively. The fluorescent PS beads in this figure were bought from Thermo Fisher Scientific.

chemically resistant characteristic, other studies also found that the acid digestion can disrupt its morphology and structure probably due to the strong oxidation and corrosion (Lusher et al., 2017), it was consistent with our results shown in the SEM images (Fig. 6B–D). The acid digestion for the MPs was too aggressive, resulting in a much lower extraction efficiency of about 4% (Avio et al., 2015). Moreover, the acid-digestion induced new functional groups such as C═O and O—H, and characteristic absorption peak of the outward bending vibration of two adjacent hydrogen atoms on the para-substituted benzene ring in the surface of the extracted fluorescent PS beads, and stretching modes for phenyl rings at ~1601 cm^{-1} disappeared (Fig. 5). These new functional groups may be generated by the strong oxidation of the concentrated acids. These changes of the surface morphology and functional groups in fluorescent PS beads induced by the digestion could disturb their characterization, thus affect the accuracy of qualitative and quantitative analysis of fluorescent PS beads in the biological samples (Andrady, 2011; Renner et al., 2017). Moreover, H_2O_2 and NaOH solution had been demonstrated to digest biogenic materials to collect MPs ingested by the organisms (Li et al., 2015; Dehaut et al., 2016; Karami et al., 2017). However, scratches and aggregates appeared on the surface of fluorescent PS beads after H_2O_2- and NaOH-digestion (Fig. 6E–F). It was reported that a part of MPs were lost when digested by H_2O_2 because of the generation of heat (Munno et al., 2018). And Cole et al., 2014 also showed that NaOH-digestion caused partial destruction of nylon fibres and melding of polyethylene fragments because the corrosive of NaOH. Besides, Rist et al. (2017) stated that the digestion using H_2O_2 and NaOH solution resulted in strong agglomeration of fluorescent PS beads. In contrast, no changes on the morphology and composition of the fluorescent PS beads after KOH-digestion in our study (Fig. 6G) confirmed the feasibility and credibility of the KOH-digestion for extracting and quantifying fluorescent PS beads from biological samples. Consistently, Dehaut et al. (2016) reported that KOH-digestion (10%w/v, 60 °C, 24 h) led to an efficient degradation of biomass but no significant effect on polystyrene particles.

4.2. Effect of digestion methods on fluorescence intensities of the fluorescent PS beads

The fluorescent PS beads were mainly produced by wrap the fluorescent materials inside of the PS shell to produce stable fluorescence (Rosenkranz et al., 2009; Zhang and Dragan, 2009). The 4-chloro-7-nitro-benzofurazan (NBD-Cl), a commonly used fluorescent dye which had no fluorescent itself, could produce a fluorescent product when it reacted with amines (Maroulis et al., 2008). Therefore, the reduction of fluorescence intensities of fluorescent PS beads probably resulted from the following two aspects. On the one hand, strong aggregations appeared among the fluorescent PS beads after digestion (Fig. 6B–F), which was consistent with the results reported by Rist et al. (2017), leading to a decrease of the fluorescence intensity. On the other hand, the digestion reagents such as HNO_3, HNO_3:HCl, and HNO_3:$HClO_4$ might react with the C—N bonds in the fluorescent materials that were formed by amine and NBD-Cl, weakening or quenching the fluorescence intensity of fluorescent PS beads. For example, NBD-Cl yield the yellow fluorescence when reacted with lisinopril (with amines) in alkaline medium (El-Emam et al., 2004). Dang et al. (2002) also demonstrated that the C—N bond was easy to fracture under the attack of HNO_3. Overall, KOH was the suitable digestion reagent for extracting fluorescent PS beads in biological samples, because it neither destroyed the surface morphology of the fluorescent PS beads (Fig. 6G)

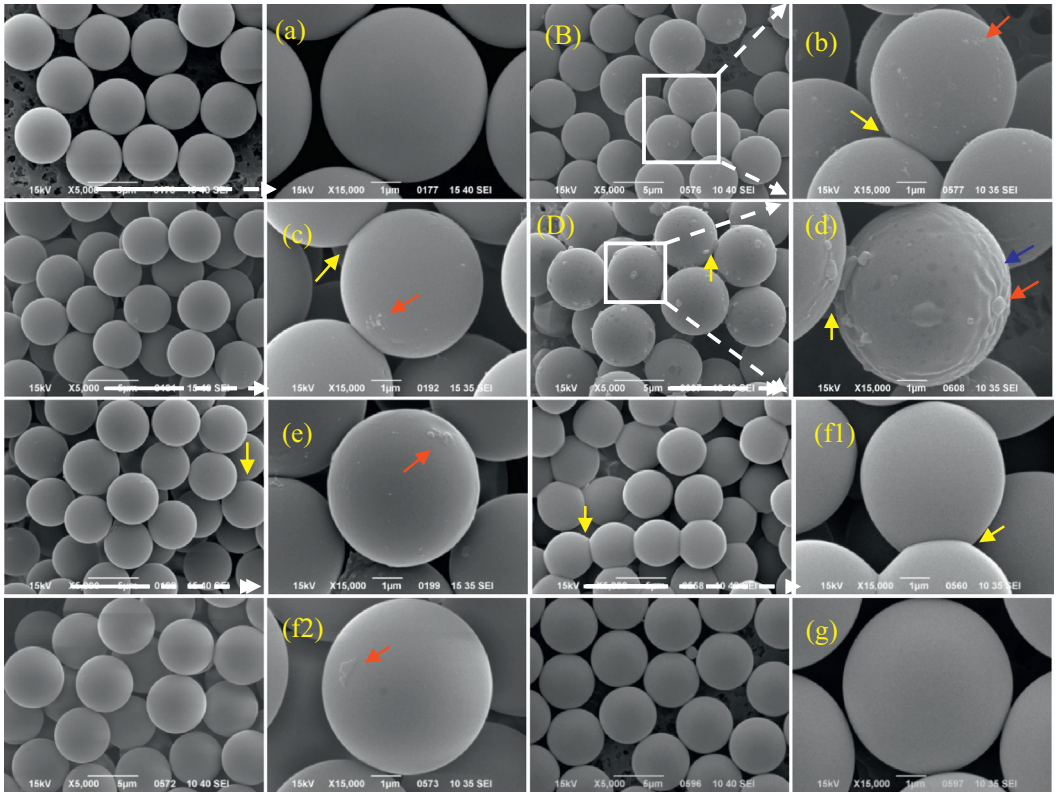

Fig. 6. SEM images of the pristine fluorescent PS beads (A) and the digested fluorescent PS beads using HNO_3 (B); HNO_3:HCl (C); HNO_3: $HClO_4$ (D); H_2O_2 (E); NaOH (F1 and F2); and KOH (G), respectively. The fluorescent PS beads were bought from Thermo Fisher Scientific. The digestion conditions were shown in Table 1. The images of (a–g) were enlarged from the frames in the images of (A–G), respectively. Compared with the pristine fluorescent PS beads (A), a series of mechanical damages were appeared on the surface of the fluorescent PS beads after the acid-digestion using HNO_3 (B); HNO_3:HCl (C) and HNO_3:$HClO_4$ (D), respectively, such as agglomeration (the yellow arrows), bubbles (the red arrows), shallow scratches, and deep depressions (the blue arrow). Slight damages and aggregations appeared on the surface of fluorescent PS beads digested using H_2O_2 (E) and strong aggregations appeared on the surface of fluorescent PS beads by NaOH-digestion (F1). Clearly, no changes were observed for the fluorescent PS beads digested by KOH-digestion (G). (For interpretation of the references to color in this figure legend, the reader is referred to the web version of this article.)

Table 2
The extraction efficiency (%) of the fluorescent PS beads in the biological samples using the optimal KOH-digestion protocol.

Samples[a]	Extraction efficiency (%)	
	Zebrafish	*D. magna*
FMPs-M	99.5 ± 0.9 a[b]	99.6 ± 0.7 a
FMPs-I	95.7 ± 0.2 b	95.3 ± 0.2 b

[a] The fluorescent PS beads were bought from Thermo Fisher Scientific (MA, USA). FMPs-M indicated the fluorescent PS beads mechanically mixed with the zebrafish or *D. magna*; FMPs-I indicated the fluorescent PS beads ingested by the zebrafish or *D. magna* during the exposure test.

[b] Different small letters indicated significant difference between the treatments that the fluorescent PS beads mechanically mixed with the organisms and the fluorescent PS beads ingested by the zebrafish or *D. magna*.

nor reacted with the amine groups of the fluorescent materials.

4.3. Effect of digestion temperature and duration time on the fluorescence intensities of fluorescent PS beads

The digestion temperature was the key parameters for chemical digestion (Munno et al., 2018). In the present study, the temperature had different effects on the fluorescence intensities of fluorescent PS beads digested by the six methods (Fig. 3B). For the acid-digestion, the fluorescence intensity significantly decreased at 20 °C and continued to decrease with increasing temperature. Enders et al. (2017) also reported that the polystyrene microbeads were subjected to stain or fading when immersed in the mixture (4:1, v/v) of HNO_3 (69%):$HClO_4$ (70%) even at room temperature. The fluorescence intensity decreased a little after alkali-digestion when the temperature was below 70 °C. And Dehaut et al. (2016) showed the organic matter could be quickly and thoroughly removed at 60 °C, leading to little effect on the MPs. However, the fluorescence intensity obviously decreased when the temperature reached 80 °C or above, probably due to this higher temperature was very closed to the glass transition temperature (95 °C) of polystyrene, at which the polystyrene particles become soft and melt together (Claessens et al., 2013).

Among the six digestion methods, the duration time had no effects on the fluorescence intensities of the fluorescent PS beads except for H_2O_2-digestion (Fig. 3B). In the H_2O_2-digestion, the fluorescence intensity of the fluorescent PS beads decreased with the increase of duration time from 10 min to 72 h indicating that H_2O_2 was not suitable for a long time digestion (Zhao et al., 2017). This was probably resulted from the strong oxidation and the release of heat during the reaction (Munno et al., 2018).

5. Conclusion

Among the six published digestion procedures, the KOH-digestion had no effect on the fluorescence intensity, surface morphology and composition of fluorescent PS beads. The KOH-digestion was slightly affected by the digestion reagent volumes, digestion temperature, and duration time. Moreover, the extraction efficiency of the fluorescent PS beads in *D. magna* or zebrafish using the KOH-digestion was

≥95.3 ± 0.2%, further confirming that the KOH-digestion is an optimal protocol with little negative impact and high extraction efficiency for extracting fluorescent PS beads from the biological samples. The other five digestion methods significantly decreased fluorescent PS beads fluorescence intensity due to agglomerations, bubbles, shallow scratches, and deep depressions, and were not suitable for extracting fluorescent PS beads from biological matrices.

Acknowledgements

This study was supported by the NSFC-Shandong Joint Fund for Marine Ecology and Environmental Sciences (no. U1606404), National Key Basic Research Program of China (2015CB453301).

Appendix A. Supplementary data

Supplementary data to this article can be found online at https://doi.org/10.1016/j.marpolbul.2018.04.056.

References

Andrady, A.L., 2011. Microplastics in the marine environment. Mar. Pollut. Bull. 62, 1596–1605.
Avio, C.G., Gorbi, S., Regoli, F., 2015. Experimental development of a new protocol for extraction and characterization of microplastics in fish tissues: first observations in commercial species from Adriatic Sea. Mar. Environ. Res. 111, 18–26.
Barboza, L.G.A., Vieira, L.R., Branco, V., Figueiredo, N., Carvalho, F., Carvalho, C., Guilhermino, L., 2018. Microplastics cause neurotoxicity, oxidative damage and energy-related changes and interact with the bioaccumulation of mercury in the European seabass, *Dicentrarchus labrax* (Linnaeus, 1758). Aquat. Toxicol. 195, 49–57.
Barnes, D.K.A., Galgani, F., Thompson, R.C., et al., 2009. Accumulation and fragmentation of plastic debris in global environments. Philos. T. R. Soc. B. 364, 1985–1998.
Batel, A., Linti, F., Scherer, M., Erdinger, L., Braunbeck, T., 2016. Transfer of benzo [a] pyrene from microplastics to *Artemia* nauplii and further to zebrafish via a trophic food web experiment: CYP1A induction and visual tracking of persistent organic pollutants. Environ. Toxicol. Chem. 35, 1656–1666.
Claessens, M., Van, C.L., Vandegehuchte, M.B., Janssen, C.R., 2013. New techniques for the detection of microplastics in sediments and field collected organisms. Mar. Pollut. Bull. 70, 227–233.
Cole, M., Lindeque, P., Fileman, E., Halsband, C., Goodhead, R., Moger, J., Galloway, T.S., 2013. Microplastic ingestion by zooplankton. Environ. Sci. Technol. 47, 6646–6655.
Cole, M., Webb, H., Lindeque, P.K., Fileman, E.S., Halsband, C., Galloway, T.S., 2014. Isolation of microplastics in biota-rich seawater samples and marine organisms. Sci. Rep. 4, 4528–4535.
Cui, X., Zhu, L., Wu, J., Hou, Y., Wang, P., Wang, Z., Yang, M., 2015. A fluorescent biosensor based on carbon dots-labeled oligodeoxyribonucleotide and graphene oxide for mercury (II) detection. Biosens. Bioelectron. 63, 506–512.
Dang, W., Kubouchi, M., Yamamoto, S., Sembokuya, H., Tsuda, K., 2002. An approach to chemical recycling of epoxy resin cured with amine using nitric acid. Polymer 43, 2953–2958.
De, W.B., Devriese, L., Bekaert, K., Hoffman, S., Vandermeersch, G., Cooreman, K., Robbens, J., 2014. Quality assessment of the blue mussel (Mytilus edulis): comparison between commercial and wild types. Mar. Pollut. Bull. 85, 146–155.
Dehaut, A., Cassone, A., Frère, L., Hermabessiere, L., Himber, C., Rinnert, E., Rivière, G., Lambert, C., Soudant, P., Huvet, A., Duflos, G., Paul-Pont, I., 2016. Microplastics in seafood: benchmark protocol for their extraction and characterization. Environ. Pollut. 215, 223–233.
Desforges, J.P., Galbraith, M., Dangerfield, N., Ross, P.S., 2014. Widespread distribution of microplastics in subsurface seawater in the NE Pacific ocean. Mar. Pollut. Bull. 79, 94–99.
El-Emam, A.A., Hansen, S.H., Moustafa, M.A., El-Ashry, S.M., El-Sherbiny, D.T., 2004. Determination of lisinopril in dosage forms and spiked human plasma through derivatization with 7-chloro-4-nitrobenzo-2-oxa-1, 3-diazole (NBD-Cl) followed by spectrophotometry or HPLC with fluorimetric detection. J. Pharmaceut. Biomed. 34, 35–44.
Enders, K., Lenz, R., Beer, S., Stedmon, C.A., 2017. Extraction of microplastic from biota: recommended acidic digestion destroys common plastic polymers. ICES J. Mar. Sci. 74, 326–331.
Geyer, R., Jambeck, J.R., Law, K.L., 2017. Production, use, and fate of all plastics ever made. Sci. Adv. 3, e1700782.
Ivar, J.A., Costa, M.F., 2014. The present and future of microplastic pollution in the marine environment. Environ. Pollut. 185, 352–364.
Jambeck, J.R., Geyer, R., Wilcox, C., Siegler, T.R., Perryman, M., Andrady, A., Narayan, R., Law, K.L., 2015. Plastic waste inputs from land into the ocean. Science 347, 768–771.
Kanhai, L.D.K., Officer, R., Lyashevska, O., Thompson, R.C., O'Connor, I., 2017. Microplastic abundance, distribution and composition along a latitudinal gradient in the Atlantic Ocean. Mar. Pollut. Bull. 115, 307–314.
Karami, A., Golieskardi, A., Choo, C.K., Romano, N., Ho, Y.B., Salamatinia, B., 2017. A high-performance protocol for extraction of microplastics in fish. Sci. Total Environ. 578, 485–494.
Li, J.N., Yang, D.Q., Li, L., Jabeen, K., Shi, H.H., 2015. Microplastics in commercial bivalves from China. Environ. Pollut. 207, 190–195.
Lu, Y., Zhang, Y., Deng, Y., Jiang, W., Zhao, Y., Geng, J., Ding, L., Ren, H., 2016. Uptake and accumulation of polystyrene microplastics in zebrafish (*Danio rerio*) and toxic effects in liver. Environ. Sci. Technol. 50, 4054–4060.
Luís, L.G., Ferreira, P., Fonte, E., Oliveira, M., Guilhermino, L., 2015. Does the presence of microplastics influence the acute toxicity of chromium (VI) to early juveniles of the common goby (*Pomatoschistus microps*)? A study with juveniles from two wild estuarine populations. Aquat. Toxicol. 164, 163–174.
Luo, L., Dai, Y., Yuan, Y., Wang, X., Liu, X., 2017. Control of head/tail isomeric structure in polyimide and isomerism-derived difference in molecular packing and properties. Macromol. Rapid Commun. 38, 1–5.
Lusher, A.L., Welden, N.A., Sobral, P., Cole, M., 2017. Sampling, isolating and identifying microplastics ingested by fish and invertebrates. Anal. Methods 9, 1346–1360.
Maroulis, M., Monemvasios, I., Vardaka, E., Rigas, P., 2008. Determination of domoic acid in mussels by HPLC with post-column derivatization using 4-chloro-7-nitrobenzo-2-oxa-1, 3-diazole (NBD-Cl) and fluorescence detection. J. Chromatogr. B 876, 245–251.
Munno, K., Helm, P.A., Jackson, D.A., Rochman, C., Sims, A., 2018. Impacts of temperature and selected chemical digestion methods on microplastic particles. Environ. Toxicol. Chem. 37, 91–98.
Noren, F., Naustvoll, L.J., 2010. Survey of Microscopic Anthropogenic Particles in Skagerrak. Report Commissioned by Klimaog Forurensningsdirektoratet, Norway.
Obbard, R.W., Sadri, S., Wong, Y.Q., Khitun, A.A., Baker, I., Thompson, R.C., 2014. Global warming releases microplastic legacy frozen in Arctic Sea ice. Earths Future 2, 315–320.
Ogata, Y., Takada, H., Mizukawa, K., Hirai, H., Iwasa, S., Endo, S., Mato, Y., Saha, M., Okuda, K., Nakashima, A., Murakami, M., Zurcher, N., Booyatumanondo, R., Zakaria, M.P., Dung, L.Q., Gordon, M., Miguez, C., Suzuki, S., Moore, C., Karapanagioti, H.K., Weerts, S., McClurg, T., Burres, E., Smith, W., Velkenburg, M.V., Lang, J.S., Lang, R.C., Laursen, D., Danner, B., Stewardson, N., Thompson, R.C., 2009. International pellet watch: global monitoring of persistent organic pollutants (POPs) in coastal waters. 1. Initial phase data on PCBs, DDTs, and HCHs. Mar. Pollut. Bull. 58 (3.146), 1437–1446.
Rebollar, E., Frischauf, I., Olbrich, M., Peterbauer, T., Hering, S., Preiner, J., Hinterdorfer, P., Romanin, C., Heitz, J., 2008. Proliferation of aligned mammalian cells on laser-nanostructured polystyrene. Biomaterials 29, 1796–1806.
Renner, G., Schmidt, T.C., Schram, J., 2017. A new chemometric approach for automatic identification of microplastics from environmental compartments based on FT-IR spectroscopy. Anal. Chem. 89, 12045–12053.
Rist, S., Baun, A., Hartmann, N.B., 2017. Ingestion of micro- and nanoplastics in *Daphnia magna* — quantification of body burdens and assessment of feeding rates and reproduction. Environ. Pollut. 228, 398–407.
Rosenkranz, P., Chaudhry, Q., Stone, V., Fernandes, T.F., 2009. A comparison of nanoparticle and fine particle uptake by *Daphnia magna*. Environ. Toxicol. Chem. (10), 2142–2149.
Sussarellu, R., Suquet, M., Thomas, Y., Lambert, C., Fabioux, C., 2016. Oyster reproduction is affected by exposure to polystyrene microplastics. P. Natl. Asad. Sci. USA. 113, 2430–2435.
Torres, F.J., Civalleri, B., Pisani, C., Musto, P., Albunia, A.R., Guerra, G., 2007. Normal vibrational analysis of a trans-planar syndiotactic polystyrene chain. J. Phys. Chem. B 111, 6327–6335.
Wang, T., Zheng, Y., Wang, X., Wang, Q., Ke, C., Austin, D.E., Han, X., Zhang, Z., 2017. Abnormal adsorption and desorption behavior of pharmaceutical drugs on polystyrene microspheres. RSC Adv. 7, 19639–19644.
Watts, A.J.R., Urbina, M.A., Goodhead, R., Moger, J., Lewis, C., Galloway, T.S., 2016. Effect of microplastic on the gills of the shore crab *Carcinus maenas*. Environ. Sci. Technol. 50, 5364–5369.
Wright, S.L., Thompson, R.C., Galloway, T.S., 2013. The physical impacts of microplastics on marine organisms: a review. Environ. Pollut. 178, 483–492.
Yang, D., Huang, W., Qiu, X., Lou, H., Qian, Y., 2017. Modifying sulfomethylated alkali lignin by horseradish peroxidase to improve the dispersibility and conductivity of polyaniline. Appl. Surf. Sci. 426, 287–293.
Yu, H., Zhao, Y., Zhou, C., Shang, L., Peng, Y., Cao, Y., Wu, L., Tung, C., Zhang, T., 2014. Carbon quantum dots/TiO_2 composites for efficient photocatalytic hydrogen evolution. J. Mater. Chem. A 2, 3344–3351.
Zhang, Y., Dragan, A., Chris, 2009. Wavelength dependence of metal-enhanced fluorescence. J. Phys. Chem. C 113, 12095–12100.
Zhao, S., Danley, M., Ward, J.E., Li, D., Mincer, T.J., 2017. An approach for extraction, characterization and quantitation of microplastic in natural marine snow using Raman microscopy. Anal. Methods 9, 1470–1478.